Biomedicine & Pharmacotherapy 141 (2021) 111921

Contents lists available at ScienceDirect

Biomedicine & Pharmacotherapy

journal homepage: www.elsevier.com/locate/biopha

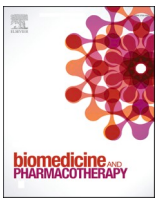

L-ergothioneine and its combination with metformin attenuates renal dysfunction in type-2 diabetic rat model by activating Nrf2 antioxidant pathway

Ayobami Dare *, Mahendra L. Channa, Anand Nadar

Department of Physiology, School of Laboratory Medicine and Medical Sciences, College of Health Sciences, University of KwaZulu-Natal, Westville Campus, Durban X54001, South Africa

ARTICLE INFO

Keywords:
Diabetes
L-ergothioneine
Metformin
Kidney
Antioxidants
Cytoprotection

ABSTRACT

L-ergothioneine (L-egt) is a bioactive compound recently approved by the food and drug administration as a supplement. L-egt exerts potent cyto-protective, antioxidant and anti-inflammatory properties in tissues exposed to injury, while metformin is a first-line prescription in type-2 diabetes. Therefore, the present study investigated the protective effect of L-egt alone, or combined with metformin, on renal damage in a type-2 diabetic (T2D) rat model. T2D was induced in male Sprague-Dawley rats using the fructose-streptozotocin rat model. L-egt administration, alone or combined with metformin, began after confirming diabetes and was administered orally for seven weeks. After the experiment, all animals were euthanized by decapitation, blood samples were collected, and both kidneys were excised. Biochemical analysis, Enzyme-link Immunoassay (ELISA), Reverse transcriptase quantitative polymerase chain reaction (RT-qPCR), western blotting, and histological analyses were done to evaluate various biomarkers and structural changes associated with renal damage. Untreated diabetic rats showed loss of kidney functions characterized by increased serum creatinine, blood urea nitrogen, proteinuria, triglycerides, lipid peroxidation, inflammation, and decreased antioxidant enzymes. Histological evaluation showed evidence of fibrosis, mesangial expansion, and damaged basement membrane in the nephrons. However, L-egt alleviates these functional and structural derangements in the kidney, while co-administration with metformin reduced hyperglycemia and improves therapeutic outcomes. Furthermore, L-egt treatment significantly increased the expression of major antioxidant transcription factors, cytoprotective genes and decreased the expression of inflammatory genes in the kidney. Thus, combining L-egt and metformin may improve therapeutic efficacy and be used as an adjuvant therapy to alleviate renal damage in type-2 diabetes.

1. Introduction

Type-2 diabetes (T2D) is a metabolic disorder exerting a heavy toll on both the individual and society with several complications, including nephropathy [39]. Diabetic nephropathy (DN) is a major microvascular complication that causes chronic kidney disease (CKD) and eventually leading to end-stage renal disease (ESRD) requiring renal hemodialysis therapy or kidney transplant [50,70]. DN develops in approximately 30–40% of patients with diabetes and progresses with time, characterized by increased urinary albumin excretion, decreased glomerular filtration rate (GFR), and increased peripheral arterial blood pressure [11,63]. The pathogenesis of DN in T2D involves a complex and multifactorial process resulting from hyperglycemia and insulin resistance (IR). The persistent hyperglycemia generates excess free radicals (e.g., ROS) that overwhelms the antioxidant defense system, resulting in oxidative injury that promotes renal inflammation and mitochondrial dysfunction [6,38]. Insulin resistance also causes dyslipidemia associated with progressive loss of renal functions via transforming growth factor- β (TGF-β) signaling pathway [27,41]. These biochemical processes stimulate different cellular signals that damage vital biomolecules and cellular components of the kidney (including DNA, proteins, podocyte, mesangial and tubular cells), exerting significant abnormalities on renal structure and function with subsequent ESRD [65]. Therefore, the prevention and management of DN should be

* Correspondence to: Discipline of Physiology, School of Laboratory Medicine and Medical Sciences, College of Health Sciences, University of KwaZulu-Natal, Westville Campus, Durban X54001, South Africa.
E-mail address: 218084517@stu.ukzn.ac.za (A. Dare).

https://doi.org/10.1016/j.biopha.2021.111921

Available online 30 July 2021

multi-targeted, focusing on cellular and molecular switches involved in the pathogenesis of DN.

The significant role of increased ROS activity in DN calls for a refined approach to antioxidant therapy, with several reports supporting the hypothesis that bioactive compounds with potent antioxidant activities can delay the development and halt the progression of DN [4,7]. L-ergothioneine (2-mercaptohistidinetrimethylbetaine) is a bioactive compound obtained solely from diets (such as mushroom, black bean, red beans, and certain meat products) and recently approved by the Foods and Drugs Administration (FDA) and European Food Safety Authority (EFSA) to be used as supplements [60,66]. L-egt (as shown in Fig. 1) possesses antioxidant and anti-inflammatory properties, while its accumulation at the sites of tissue injury has been hypothesized as an adaptive mechanism of protecting tissues at risk of damage and regenerating injured tissues [21,42]. Also, L-egt has been reported to activate the Nrf2 (nuclear factor erythroid-2 related factor-2) antioxidant signaling pathway to protect against cellular injury, enhance glutathione level and reduce oxidative damage in the kidney as well as activates sirt1 and 6 to protect against high glucose-induced cell senescence [12,13,22]. Furthermore, coadministration of L- egt with existing therapy (such as melatonin and hispidin) significantly increases treatment benefits both in-vitro and in-vivo [52,53], suggesting that L-egt may improve the efficacy of available treatment options. In addition, it has been shown that the reno-protective effect of metformin goes beyond its antihyperglycemic effect; metformin alleviates oxidative stress, suppresses TGF-β1 inflammatory pathway, and attenuates apoptosis [47,69]. However, the effect of L-egt and its co-administration with metformin against renal complications associated with diabetes is yet to be established. Thus, this study was designed to investigate the effect of L-egt, with or without metformin, on renal dysfunctions associated with diabetes in a rat model of type-2 diabetes.

2. Materials and methods

2.1. Drugs and chemicals

Pure L-ergothioneine was sponsored by Tetrahedron (Paris, France www.tetrahedron.fr). Streptozotocin (STZ) was obtained from Sigma-Aldrich (St., Louis, MO, USA). Acucheck glucose strips and metformin (Austell Laboratories Pvt. Ltd.) were purchased from Pharmed Ltd., (Durban, South Africa). Fructose (Radchem (PTY) Ltd) was purchased from Laboquip (Durban, South Africa). All chemicals and reagents used in this study were analytical grades and available commercially.

2.2. Animals

Thirty-six (36) adult male Sprague-Dawley rats weighing (175 ± 20) g were used in this study. The animals were obtained from the Biomedical Research Unit (BRU), Westville Campus, University of KwaZulu-Natal, Durban, South Africa. The animals were allowed to acclimatize to standard laboratory conditions (temperature 23 ± 1 °C, 40–60% humidity) and 12 h light-dark cycles with free access to standard rat chow (Meadow Feeds, South Africa) and water *ad libitum* for one week before the experiment. All animal protocol was done according to the National Institutes of Health guide for the care and use of laboratory animals (NIH Publications No. 8023, revised 1978) and approved by the University of KwaZulu-Natal Animal Research Ethics Committee, Durban, South Africa, with ethical clearance (AREC/006/019D).

2.2.1. Induction of experimental diabetes

Type-2 diabetes rat model was induced using fructose plus a low dose of streptozotocin model reported previously by [68]. Briefly, after acclimatization, the animals were randomly divided into two major groups: non-diabetic (n = 12) and diabetic groups (n = 24). The diabetic group was supplied with 10% fructose solution *ad libitum* in drinking water for 14 days to induce insulin resistance, while the non-diabetic groups were supplied with distilled water. After 14 days, all animals were fasted for 8–10 h before intraperitoneal injections. The diabetic groups were injected a single low dose of streptozotocin (STZ) (40 mg/kg *bwt*) dissolved in freshly prepared 0.1 M citrate buffer (pH 4.5), while the non-diabetic groups were injected with the same volume of citrate-buffer only. One week after STZ injection, non-fasting blood glucose (NFBG) levels were measured in all animals using a portable glucometer Accu-Chek Active (Roche Diagnostics GnbHD-68298 Mannheim, Germany) in the blood collected from the tail vein. Animals with NFBG levels > 16.7 mmol/L were considered diabetic [54] and included in the study.

2.3. Experimental protocol

After the induction of diabetes, non-diabetic rats were subdivided into two groups, and the diabetic rats were randomly divided into four groups (n = 6) and treated as follows.

- Non-diabetic control (NC) - 1 ml/100 g bwt of distilled water.
- Diabetes control (DC) - 1 ml/100 g bwt of distilled water.
- Diabetes + L-egt (DE) - 35 mg/kg bwt of L-egt.
- Diabetes + metformin (DM) - 500 mg/kg bwt of metformin.
- Diabetes + L-egt + metformin (DEM).

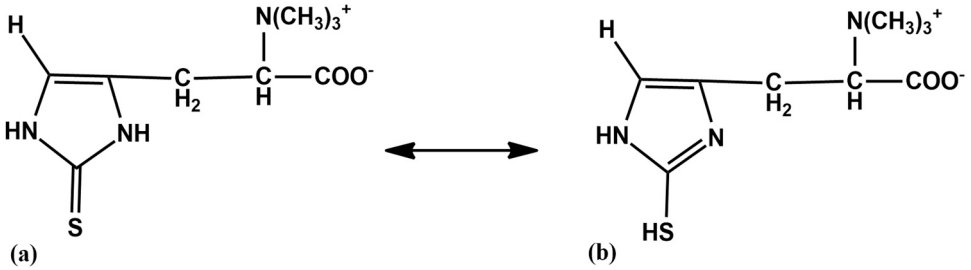

Fig. 1. Chemical structure of thione-thiol tautomers of L-ergothioneine. In solution at physiological pH, L-egt exists predominantly in the thione (a) rather than the thiol (b) [21].

Distilled water, L-egt, and metformin were administered orally for seven weeks after confirmation of diabetes. In addition, body weight was recorded every week. Dosage of L-egt was selected based on distribution and accumulation of dietary ergothioneine in mouse tissues and in accordance with previous studies that used this nutraceutical [56, 67].

2.4. Collection of samples

After seven weeks of treatment, the animals were placed individually in a metabolic cage for 24 h to measure water intake and collect urine samples using a sterile container. Urine volume was recorded, and the collected samples were centrifuged at 2000 rpm, 10 mins at 4 °C to remove any suspended particles. The urine samples were then aliquoted in Eppendorf tubes and stored at − 20 °C until analysis. Rats were sacrificed by decapitation, and blood samples were collected into a serum vacutainer bottle; centrifuged at 3000 rpm for 10 mins to obtain serum and stored in the bio-freezer at − 80 °C until used for analysis. The kidneys were rapidly excised, cleaned of adhering tissues, weighed, and rinsed in cold saline. The right kidney was rapidly frozen in liquid nitrogen and stored at − 80 °C until used for analysis, while the left kidney was fixed in 10% neutral-buffered formalin histopathological analysis.

2.4.1. Preparation of kidney homogenates

The kidney samples were thawed and homogenized in 10% phosphate buffer (0.1 M, pH7.4). The homogenates were vortexed and centrifuged at 600 g for 10 min to remove cell debris. The supernatant was subsequently centrifuged at 10,000 g for 20 mins to obtain the cytosolic fraction and used for biochemical analyses.

2.5. Assessment of body weight, kidney weight, and blood glucose

The bodyweight of all animals was recorded weekly. The kidney index was assessed by calculating the kidney-to-bodyweight ratio. Non-fasting blood glucose levels were recorded before and after the experiment using a glucometer (Accu-Chek Performa, USA).

2.6. Biochemical analysis

Serum and urine samples were analyzed at Global clinical and viral laboratories (Amanzimtoti, South Africa) for quantification of serum creatinine (Scr), Blood Urea Nitrogen (BUN), and Urinary albumin (Ualb), Urine creatinine (Ucr), and triglyceride (TG) using a biochemical analyzer. Urine protein was quantified by Bradford assay (Sigma Aldrich Chemical Company, Missouri, and St Louis, USA). The renal index was estimated by calculating the ratio of kidney weight to body weight. Creatinine clearance was used to estimate glomerular filtration rate and was calculated using the formula:

$$\mathrm{Ccr(ml/min)} = \frac{\text{Urine creatinine (mg/dl)} \times \text{urine volume (ml/24hrs)}}{\text{Serum creatinine (mg/dl)} \times 60\text{min} \times 24\text{hrs}}$$

[44].

2.6.1. Evaluation of lipid peroxidation and antioxidant enzymes

The concentration of malondialdehyde (MDA), a marker of lipid peroxidation, was evaluated by measuring the content of thiobarbituric acid (TBA) reactive product in the kidney homogenates using the protocol previously described by [36]. The concentration of antioxidant enzymes (SOD, GSH, and CAT) was also measured in the kidney homogenates by spectrophotometric assay. Reduced-GSH and SOD levels were assessed using the method [16,32]. CAT activity was analyzed following the method reported by [1].

2.6.2. Evaluation of renal inflammation and fibrosis biomarkers

Pro-inflammatory cytokine, tumor necrosis factor –α (TNF–α); chemokine, monocyte chemotactic protein-1 (MCP-1) and fibrotic cytokine, tumor growth factor-β (TGF-β) were quantified in the kidney homogenates using their specific ELISA kits (Elabscience Biotechnology Co., Ltd., Houston, TX, USA) according to the manufacturer's protocol. Absorbance was measured using the microplate reader, SPECTROstar Nano spectrophotometer (BMG LABTECH, Ortenburg, LGBW, Germany).

2.6.3. Histopathological examination of the kidney

Kidney samples were fixed in 10% neutral-buffered formalin. Specimens were then dehydrated in a graded series of ethanol cleared in xylene and embedded in paraffin wax. The samples were then cut into slices (5-μm thick) using a micron rotary microtome and stained with hematoxylin and eosin (H&E). Kidney sections were also sent to an accredited laboratory (Lancet laboratory, South Africa) for Periodic Acid Schiff (PAS) and Masson's trichome special stains. The stained sections were visualized using a nanozoomer S360 digital slide scanner (Hamamatsu Photonics, Japan) and nanozoomer digital pathology version 2.8 software for analysis by a pathologist. H&E-stained sections were used to determine the degree of damage in the kidney tissue; PAS and Masson trichome stained were used to evaluate hyperplasia in the glomerular mesangial area and renal fibrosis, respectively.

2.6.3.1. Quantitative and semiquantitative analysis of renal injury.

Quantitative analysis of tubular dilation in the H&E-stained sections and mesangial matrix expansion in the PAS-stained sections were quantified using ImageJ 1.53e analysis software (NIH, USA). Ten to twelve fields of images containing tubular structures were selected per slide to evaluate tubular dilation. The cross-sectional diameter of tubules in the selected cortical field was measured by line morphometric measurements from digital images (Olympus BX51 microscope mounted with a digital camera; Olympus Optical; Tokyo, Japan) and ImageJ 1.53e software analysis (NIH, USA) as described by [45]. To estimate the tubular diameter, the straight-line tool on the software is used to draw a straight line that passes through the center of a symmetrically sectioned tubule and joins two points on the tubular circumference [46,57]. The distance (μm) is calculated by selecting Analyze/Measure and waiting for the 'Length' to appear in the Results window. The average diameter of ten tubules is then recorded for each kidney sample, and three kidney samples were selected per group (n = 3). The mean ± sem value for each group was presented on a bar chart in Fig. 8a.

The total glomerular area and glomerular mesangial area were also analyzed with ImageJ software as previously described by [55]. Five to seven fields of images showing glomerular structures were selected per slide (n = 3/group) in the PAS-stained section at x200 magnification to measure the total glomerular area. The total glomerular image was manually selected by the polygonal selection tool from the software and extracted from the other parts of the histological slice image. The total glomerular area was measured, and the result was recorded. The selection of mesangial area in the glomerulus, which was stained purple on PAS-stained sections, was performed by the "color-based thresholding" option [51]. Afterward, only the purple-stained parts of the glomerular tuft remained on the image, further converted into binary images. The binary image was used for mesangial area measurement. The average

area of five glomerular structures is then recorded for each kidney sample, and three kidney samples were selected per group (n = 3). The mean ± sem values for each group were calculated. Then, the percentage ratio of the mesangial area to the total glomerular area was used to estimate the mesangial matrix index as presented in Fig. 8b. For semi-quantitative analysis of renal fibrosis, the percentage of collagen deposit (green stain in Trichome-stained sections) was evaluated and presented in Fig. 8c. Twenty glomeruli were randomly selected from each section, and the green stained collagen area in each glomerulus was scored by a pathologist blinded to the study using the method [26]: 0 = < 25% stained collagen area; 1 = 25–50% stained collagen area; 2 = 50–75% stained collagen area; and 3 = >75% stained collagen area.

2.6.4. Reverse transcription quantitative Polymerase Chain Reaction (RT-qPCR)

TRIzol reagent (40 mg of tissue/ml, Trizol reagent) was used to extract total RNA from the kidney. The quality and quantity of isolated RNA were evaluated by measuring absorbance at 260/280 nm with a nanodrop ND-1000 spectrophotometer (Thermo scientific, Johannesburg, South Africa). After that, iScript cDNA synthesis kit, Life Science research (Biorad, South Africa), was used to convert the RNA into cDNA according to the manufacturers' instructions.

Real-time qPCR of samples was used to determine the mRNA expression level of Nrf2, Ho-1, NQO-1, sirt1, NF-kB, TGF-β1, fibronectin, and GAPDH using iTaq Universal SYBR Green PCR master mix analysis (Biorad, CA, USA) on a light cycler 96 RT-PCR system (Roche, Mannheim, Germany). RT-qPCR was performed in a 10 μL reaction volume containing 5 μL SYBR Green Master Mix, 1 μL of each primer, 1 μL of nuclease-free water, and 2 μL of cDNA template. The primer sequences are shown in Table 1. The purity and specificity of amplified PCR products were verified by melting curves generated at the end of each PCR. Data from the real-time analysis were calculated using the v1.7 sequence detection software from PE Biosystems (Foster City, CA). Relative mRNA expression of the genes of interest was calculated using the $2^{-\Delta\Delta ct}$ method [30] and normalized in relation to the expression of the endogenous control, GAPDH. The primers sets were homology searched using an NCBI BLAST search to ensure that they were specific.

2.6.5. Western blot analysis of Nrf2 protein expression

Total protein was extracted from the kidney tissues using RIPA cell lysis buffer. Nrf2 protein expression was evaluated by western blotting technique. Beta-actin was used as the housekeeping protein. The amount of protein in the lysate was quantified using an RC DC protein assay kit (Biorad, CA, USA). An equal amount of protein was separated by electrophoresis using 8–16% SDS-PAGE (Bio-Rad, California, USA) at 100 V, 25 mA for 90 mins, and transferred to a PVDF membrane (Amersham Biosciences). After transfer, the membrane was blocked with intercept (PBS) blocking buffer (Celtic Molecular diagnostic, South Africa) for 2 h at room temperature with gentle shaking. Then, the membrane was washed with PBST and incubated overnight at 4 °C with mouse anti-Nrf2 antibody (ab89443, 1:500 dilution) and β-actin (1:2000). Next, the membrane was washed three times with PBST and later incubated with a secondary antibody, IRDye 680, 1:15,000 dilution (Li-Cor Bioscience, Lincoln, USA) in a blocking buffer containing 0.2% Tween-20 for one hour at room temperature in the dark. The protein bands were detected using an Odyssey CLx imaging system (Li-Cor Bioscience, Lincoln, United States), and the intensities were quantified using Odyssey image studio v2.1. Results were expressed as the ratio of Nrf2/β-actin.

2.7. Statistical analysis

Data were presented as the mean ± SEM and analyzed by GraphPad Prism version 7 (GraphPad, San Diego, CA) using one-way analysis of variance (ANOVA), followed by Tukey's multiple comparison tests to determine differences between groups. $P < 0.05$ was considered statistically significant.

3. Results

3.1. Effect on kidney hypertrophy, Fasting blood glucose, water intake, and triglyceride level

The effect of L-egt, with or without metformin, on kidney hypertrophy (KW/BW), blood glucose, water intake, and TG after seven weeks of treatment is presented in Fig. 2a-d. Kidney hypertrophy was expressed as a percentage ratio of kidney weight to body weight. DC animals

Table 1
Nucleotide sequence, accession number, and product size.

Genes	Primer sequence	GenBank Accession number	Product size (bp)
GAPDH	F: 5′-TTCAACGGCACAGTCAAGG-3'R: 5′-CGGCATGTCAGATCCACAA-3'	NM_017008.4	578
HO-1	F: 5′-CGACAGCATGTCCCAGGATT-3′R: 5'-TCGCTCTATCTCCTCTTCCAGG-3.'	NM_012580.2	184
NQO-1	F: 5'-CATTCTGAAAGGCTGGTTTGA-3'R: 5'-CTAGCTTTGATCTGGTTGTCG-3'	NM_017000.3	486
Nrf_2	F: 5'-GCCAGCTGAACTCCTTAGAC-3'R: 5'-GATTCGTGCACAGCAGCA -3'	NM_031789.2	466
Sirt1	F: 5'- CCCAGATCCTCAAGCCATGTTC-3'R: 5'- TGTGTGTGTGTTTTTCCCCC-3'	NM_001372090.1	119
Fibronectin	F: 5'-GTGGCTGCCTTCAACTTCTC-3'R: 5'-AGTCCTTTAGGGCGGTCAAT-3'	XM_006245158.4	231
TGFβ1	F: 5'-GGGCTACCATGCCAACTTCTG-3'R- 5'- GAGGGCAAGGACCTTGCTGTA-3'	NM_021578.2	82
NF-kB	F: 5'-ACGATCTGTTTCCCCTCATCT-3'R: 5'- TGCTTCTCTCCCCAGGAATA-3'	NM_199267.2	150

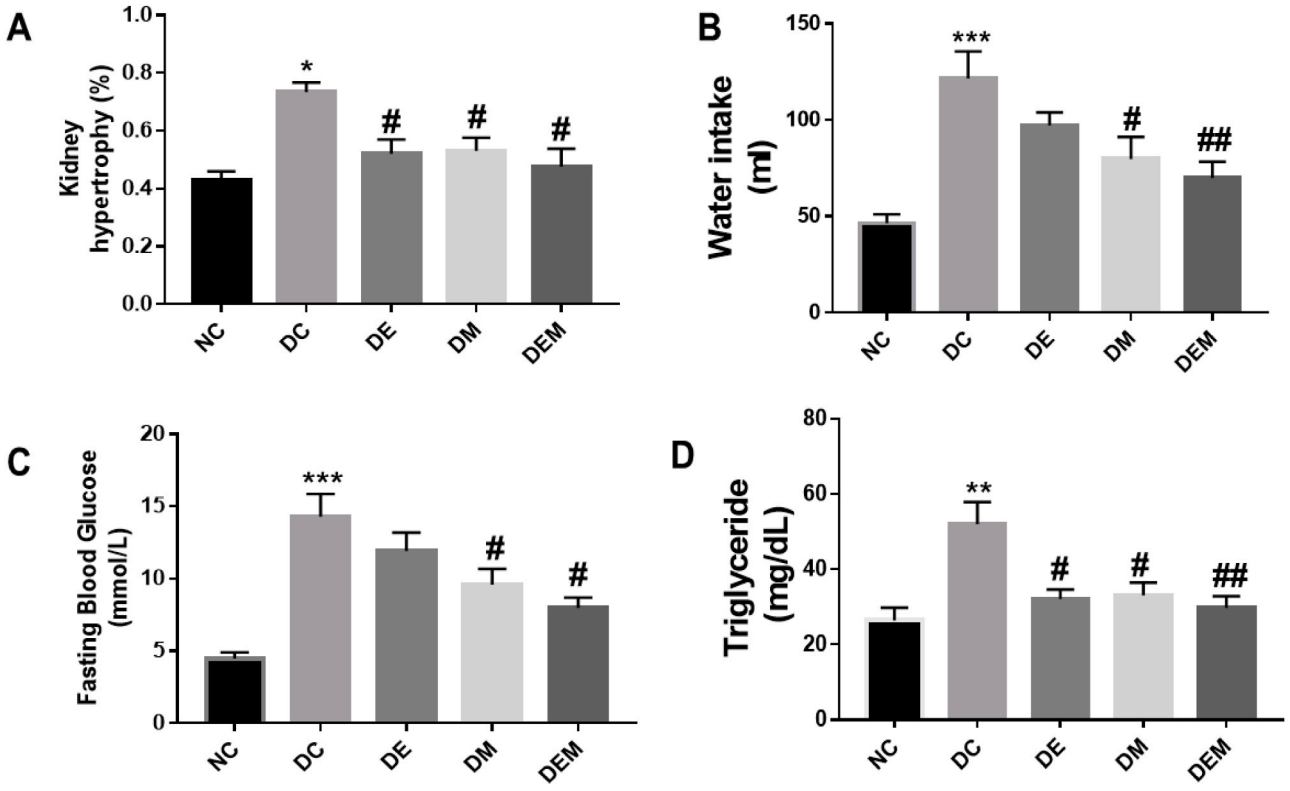

Fig. 2. a-d: Effect on kidney hypertrophy, blood glucose, water intake and triglyceride level. *P < 0.05, **p < 0.01, ***p < 0.001 vs NC while $^{\#}$p < 0.05, $^{\#\#}$p < 0.01 vs DC and $^{\$}$p < 0.05 vs DM. (n = 6). KW/BW = Kidney weight: body weight, FBG = fasting blood glucose, TG- triglycerides. Non-diabetic control (NDC), Diabetic control (DC), Diabetic treated plus L-egt only (DE), Diabetic plus metformin only (DM), Diabetic plus L-egt and metformin (DEM).

showed a significant increase ($p < 0.05$) in kidney hypertrophy vs. NC animals, while the administration of L-egt with or without metformin to diabetic rats significantly reduced ($p < 0.05$) kidney hypertrophy vs. DC rats. There was a significant increase ($p < 0.001$) in blood glucose in the DC animal vs. NC animals. While the administration of L-egt alone (DE) showed a non-significant decrease ($p > 0.05$) in blood glucose, coadministration with metformin (DEM group) caused a significant decrease in blood glucose level vs. DC rats. There was a significant increase ($p < 0.01$) in serum TG in DC animals vs. NC animals, while L-egt administration with or without metformin caused a significant reduction ($p < 0.05$) in TG level vs. DC animals.

3.2. Effect on biomarkers of renal function

The effects of L-egt treatment on biomarkers of renal function after seven weeks of administration are presented in Fig. 3a-g Serum creatinine (Scr) and blood urea nitrogen (BUN) in the DC animals significantly increased ($p < 0.01$) vs. NC animals. However, there was a significant reduction ($p < 0.05$) in these serum biomarkers after seven weeks of administering L-egt vs DC animals. Interestingly, coadministration of L-egt with metformin (DEM) caused a significant reduction ($p < 0.05$) in BUN vs diabetic rats treated with metformin only (DM). Furthermore, DC animals showed a significant increase in urinary protein ($p < 0.05$), urine albumin ($p < 0.05$), and urine volume ($p < 0.01$) vs NC animals. However, L-egt treatment, with or without metformin, to diabetic animals significantly reduced ($p < 0.05$) urine protein and albumin vs. DC, while urine volume decreased significantly ($p < 0.05$) in the DEM group vs DC group. Creatinine clearance (Ccr) decreased significantly ($p < 0.01$) in the DC vs. NC animals. Treatment with L-egt alone caused a non-significant ($p > 0.05$) increase in Ccr like metformin vs. rats, while coadministration of both drugs caused a significant ($p < 0.05$) increase in Ccr. Kidney injury molecule-1 (KIM-1) concentration in the kidney homogenates of DC animals significantly increased ($p < 0.05$) vs. NC animals. However, administration of L-egt with or without metformin to diabetic rats caused a significant decrease ($p < 0.05$) in renal KIM-1 concentration compared with DC rats.

3.3. Effect on lipid peroxidation and antioxidant biomarkers

Fig. 4a-d shows the effect of L-egt on kidney malondialdehyde (MDA), superoxide dismutase (SOD), reduced glutathione (GSH), and catalase (CAT) level in the kidney homogenates after seven weeks of treatment. There was a significant increase ($p < 0.01$) in MDA level (a marker for oxidative stress) in the DC group vs. NC group, while L-egt administration, with or without metformin, to diabetic rats, significantly reduced MDA level (DE: $p < 0.05$; DEM: $p < 0.01$) vs. DC group. In addition, antioxidant enzymes (SOD, GSH, and CAT) were significantly reduced ($p < 0.05$) in the DC group vs. NC group. However, administration of L-egt with or without metformin to diabetic rats significantly increased ($p < 0.05$) SOD and GSH level vs. DC group, while CAT level

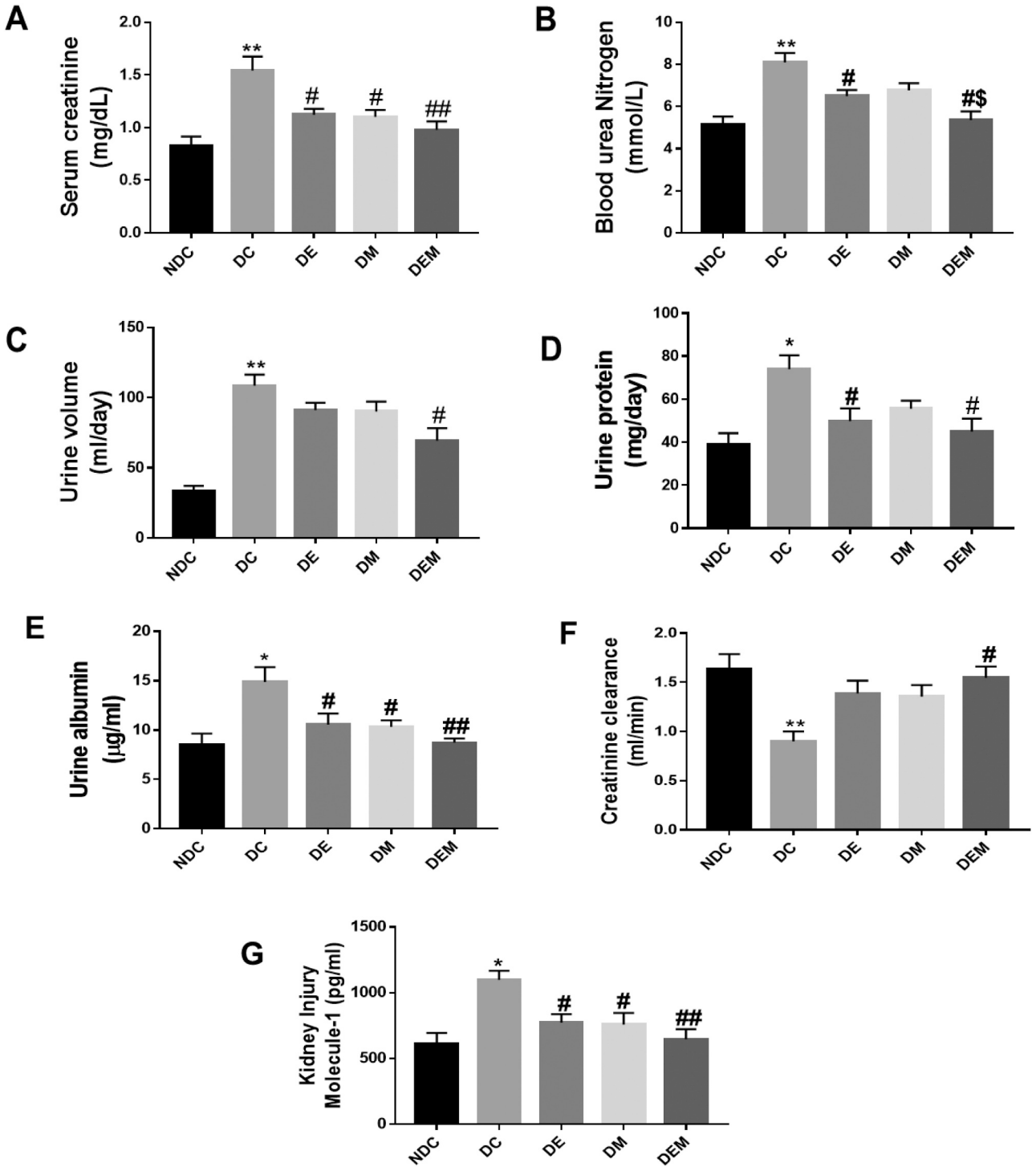

Fig. 3. a–g: Effect of L-egt alone with or without metformin on biomarkers of renal functions *p < 0.05, **p < 0.01 vs NC while $^{\#}$p < 0.05, $^{\#\#}$p < 0.01 vs DC and $^{\$}$p < 0.05 vs DM. (n = 6). (A) Serum creatinine, (B) Blood urea nitrogen, (C) urine volume, (D) urine protein, (E) urine albumin, (F) creatinine clearance, and (G) Kidney injury molecule 1. Non-diabetic control (NDC), Diabetic control (DC), Diabetic treated plus L-egt only (DE), Diabetic plus metformin (DM), Diabetic plus L-egt, and metformin (DEM).

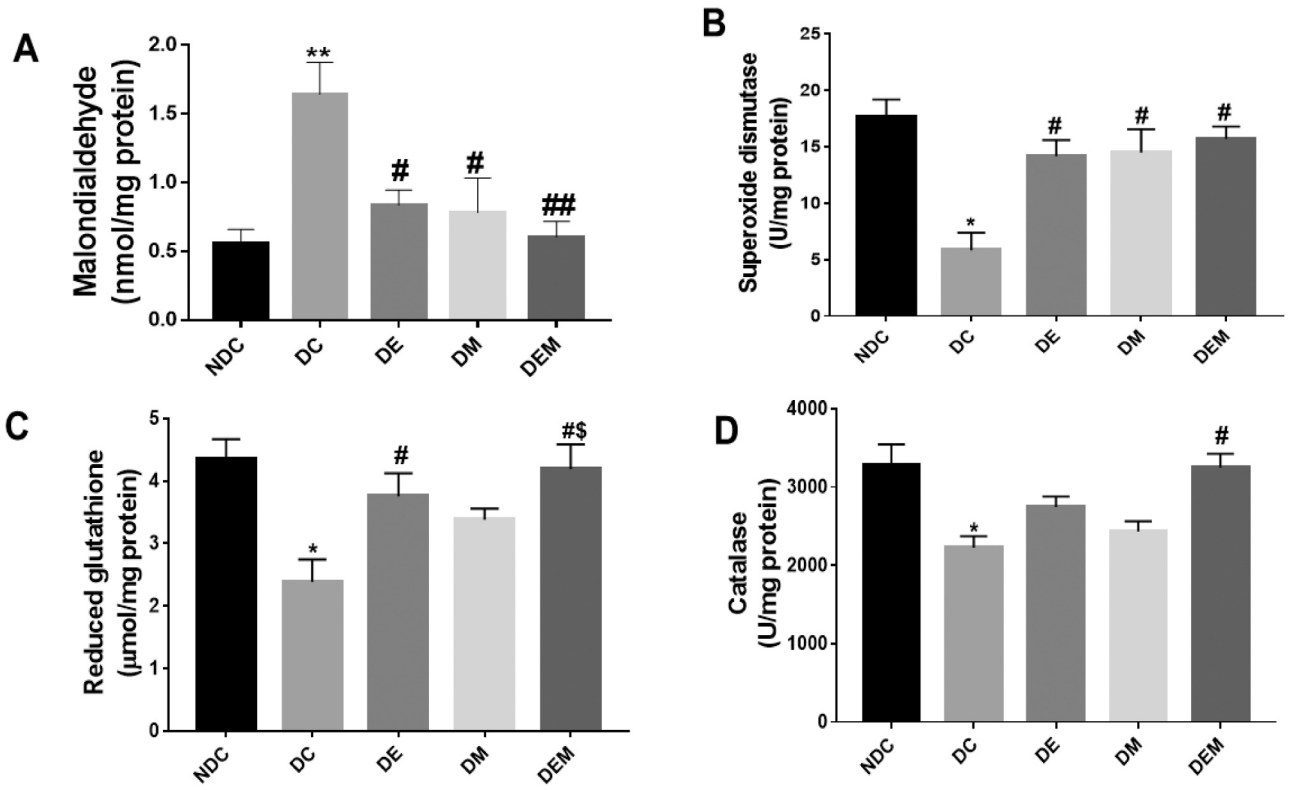

Fig. 4. a–d: Effect of L-egt alone with or without metformin on lipid peroxidation and antioxidant biomarkers. *$p < 0.05$, **$p < 0.01$ vs NC while $^{\#}p < 0.05$, $^{\#\#}p < 0.01$ vs DC and $^{\$}p < 0.05$ vs DM. (n = 6). Non-diabetic control (NC), diabetic control (DC), Diabetic treated plus L-egt only (DE), Diabetic plus metformin (DM), Diabetic plus L-egt, and metformin (DEM). (A) Malondialdehyde (MDA), (B) Superoxide dismutase (SOD), (C) Reduced glutathione (GSH), and (D) Catalase (CAT).

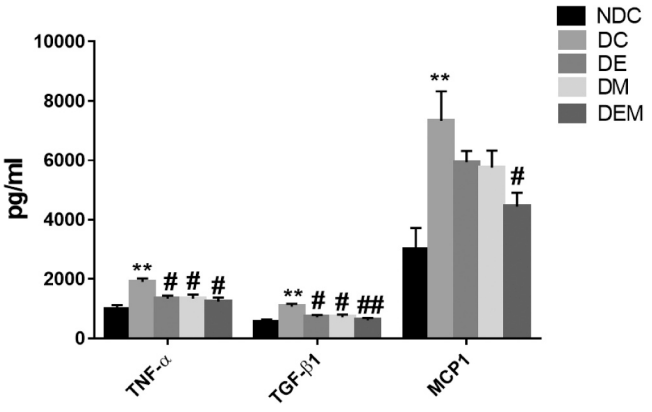

Fig. 5. Effect of L-egt with or without metformin on inflammatory biomarkers. **$p < 0.01$, vs NDC while $^{\#}p < 0.05$, $^{\#\#}p < 0.01$ vs DC. (n = 6). Non-diabetic control (NC), diabetic control (DC), Diabetic treated plus L-egt only (DE), Diabetic plus metformin (DM), Diabetic plus L-egt and metformin (DEM). TNF-α: tumor necrotic factor- α; MCP-1: monocyte chemoattractant protein-1 and TGF-β1: Transforming growth factor- β1.

significantly increased ($p < 0.05$) in the DEM group vs DC group. Interestingly, coadministration of L-egt with metformin to diabetic rats (DEM group) significantly increased ($p < 0.05$) GSH level vs. DM group.

3.4. Effect on Inflammatory biomarkers

Effects of L-egt, with or without metformin, on tumor necrotic factor-α (TNF-α), monocyte chemoattractant protein-1 (MCP-1) and Transforming growth factor (TGF-β1) level in the kidney homogenates after seven weeks of treatment is presented in Fig. 5. There was a significant increase in TNF-α, MCP-1, and TGF-β1 ($p < 0.05$) in the DC rats vs. NC rats. Conversely, L-egt administration to diabetic rats (DE) significantly reduced TNF-α and TGF-β1 levels ($p < 0.05$) with a non-significant decrease in MCP-1 level ($p > 0.05$) vs. DC rats. Interestingly, coadministration of L-egt with metformin (DEM) to diabetic animals significantly reduced inflammatory biomarkers (TNF- α: $p < 0.05$, MCP-1: $p < 0.05$; TGF- β1: $p < 0.01$) vs. DC rats.

3.5. Effect on mRNA expression of antioxidant and inflammatory transcription factors

The mRNA level of major transcription factors (e.g., Sirt1, Nrf2, HO-1, NQO-1, NF-kB, TGF- β1, and fibronectin mRNA expression) mediating the antioxidant and inflammatory signaling pathway is presented in Fig. 6a-b. The result showed that the transcriptional level of Sirt1, Nrf2, and NQO-1 reduced significantly ($p < 0.05$) in the DC group vs. NC group, while L-egt, with or without metformin, significantly increased ($p < 05$) mRNA expression of these transcription factors vs. DC. Interestingly, Coadministration of L-egt with metformin to diabetic rats (DEM group) significantly increased ($p < 0.05$) Nrf2 and HO-1 mRNA expression vs. DM group. However, the DC group showed a significant increase ($p < 0.01$) in NF-kB, TGF- β1, and fibronectin mRNA expression vs. the NC group. Administration of L-egt, with or without metformin, to

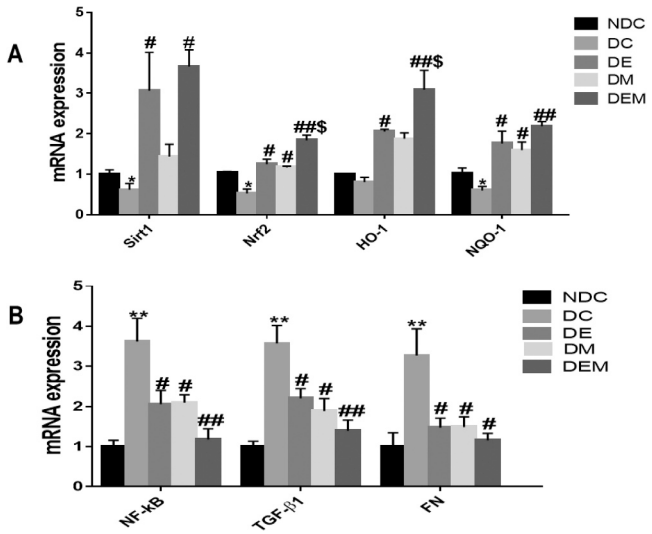

Fig. 6. a-b: Effect of L-egt with or without metformin on relative mRNA expression. $^{**}p < 0.01$, $^{*}p < 0.05$ vs NC while $^{\#}p < 0.05$, $^{\#\#}p < 0.01$ vs DC. $^{\$}p < 0.05$ vs DM. Non-diabetic control (NC), Diabetic control (DC), Diabetic treated plus L-egt only (DE), Diabetic plus metformin only (DM), Diabetic plus L-egt and metformin (DEM). Nrf2 = Nuclear factor erythroid-2 related factor-2, Sirt1 = sirtuin-1, HO1 = hemeoxygenase-1, NQO1 = NAD(P)H quinone oxidase-1, NF-kB = Nuclear factor kappa-B, TGF-β1: Transformin growth factor- β1 and FN = fibronectin.

diabetic rats significantly reduced (DE: $p < 0.05$; DEM: $p < 0.01$) mRNA expression of these inflammatory biomarkers vs. DC group.

3.6. Effect on Nrf2 protein expression

The relative protein expression of Nrf2 in the kidney is presented in Fig. 7a-b. The result showed that Nrf2 protein expression significantly decreases in the DC group Vs. NC group. L-egt, with or without metformin, significantly increased Nrf2 protein expression Vs. DC group.

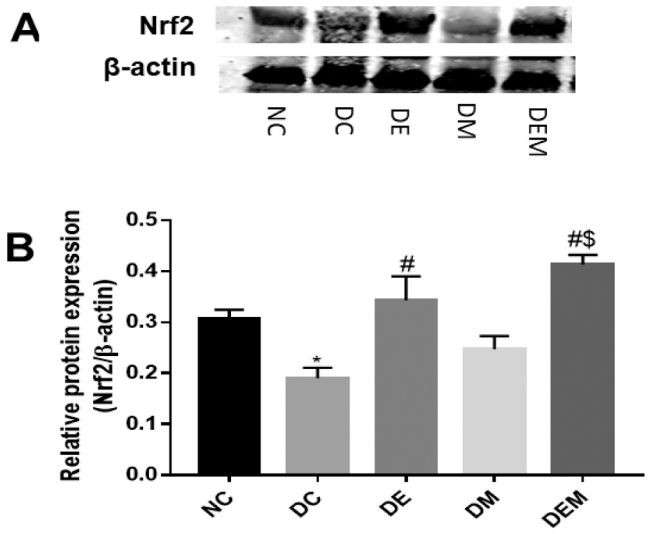

Fig. 7. a-b: Effect of L-egt with or without metformin on relative Nrf2 protein expression. $^{*}p < 0.05$ vs NC while $^{\#}p < 0.05$, vs DC. $^{\$}p < 0.05$ vs DM. Non-diabetic control (NC), diabetic control (DC), diabetic treated plus L-egt (DE), diabetic plus metformin (DM), diabetic plus L-egt, and metformin (DEM). (A) immunoblot of Nrf2 and β-actin. (B) Relative Nrf2 protein expression.

3.7. Effect on histological changes in the kidney

Histological evaluation of the kidney sections after seven weeks of administering L-egt, with or without metformin, to T2DM animals is shown in Fig. 8a–c.

4. Discussion

Recently, attention has been drawn to the use of drug adjuvants to reduce the dosage of administered drugs, minimize adverse effects, improve the efficacy of therapeutic interventions, and delay the onset or halt the progression of diabetic complications [8,25]. Thus, the present study evaluated the benefits of L-ergothioneine alone and combined with metformin in renal dysfunctions associated with T2D in an animal model. Significantly, this study shows that L-egt exerts reno-protective effects and improves therapeutic outcomes when administered with metformin, thus, providing further support to the use of combination therapies to manage diabetic nephropathy. Also, previous studies have reported that L-egt activates Nrf2 and inhibits NF-kB in several animal models [28,49]. To this end, we evaluated the beneficial role of L-egt-induced Nrf2 activation in diabetes-induced kidney disease and the result of this study is summarized as shown in Fig. 9.

In this study, the combination of L-egt and metformin improves glucose metabolism in diabetic animals, resulting from the improved efficacy of metformin to increase insulin sensitivity, thereby promoting glucose uptake and decreased hepatic gluconeogenesis by activating the AMPK pathway [2]. Increased serum triglycerides have also been reported as an independent risk factor contributing to the development of renal damage in diabetes [48,58]. Previous studies in both human and animal models have reported the lipid-lowering effect of mushrooms, attributed to the bioactive content in this food [18,34]. Thus, the reduced serum triglycerides in diabetic animals treated with L-egt suggests that this nutraceutical can alleviate risk factors associated with renal dysfunction. This result is in accordance with a previous study done by [3], where ergothioneine-rich mushroom extract reduced intracellular triglyceride level by downregulating sterol regulatory binding protein-1c (SREBP1c), and hepatic lipogenesis.

Kidney hypertrophy is well correlated with chronic hyperglycemia, resulting from excessive proliferation of mesangial cells and substantial accumulation of extracellular matrix. Kidney hypertrophy is accompanied by tubular basement membrane thickening and has been identified as an early marker of diabetic nephropathy [20,59]. The potency of L-egt to reduce kidney hypertrophy in diabetic animals suggests that this compound may inhibit mesangial cell proliferation and excessive growth of the tubular epithelial cells that contribute significantly to kidney hypertrophy, thereby preventing structural damage and loss of function in the kidney. The proximal tubular cells and the mesangial cells are the primary targets of hyperglycemia due to their inability to downregulate glucose uptake [61]. Therefore, chronic exposure to hyperglycemia and other risk factors promotes cellular injury in the kidney, resulting in compromised renal function. In this study, renal function was significantly reduced in the diabetic control animals, as shown in Fig. 3, which is similar to previous reports in the literature [10,72]. The reduced Scr, BUN, Upro, Ualb, KIM-1, and increased Ccr in diabetic rats treated with L-egt indicates that L-egt improves glomerular and tubular functions, which may be attributed to the potency of this nutraceutical to protect against cell injury and enhance the integrity of the glomerular filtration barrier. Studies have shown that metformin improves glycemic control, alleviates oxidative stress, and inhibits apoptosis diabetic nephropathy [47,71]. The combination regimen improves renal function compared to either L-egt or metformin administration alone.

Oxidative stress plays a crucial role in the development and progression of diabetic kidney disease. The altered redox balance causes oxidative injury in the renal cells, promoting fibrosis and inflammation that mediate glomerulosclerosis and tubulointerstitial injury [19,24,

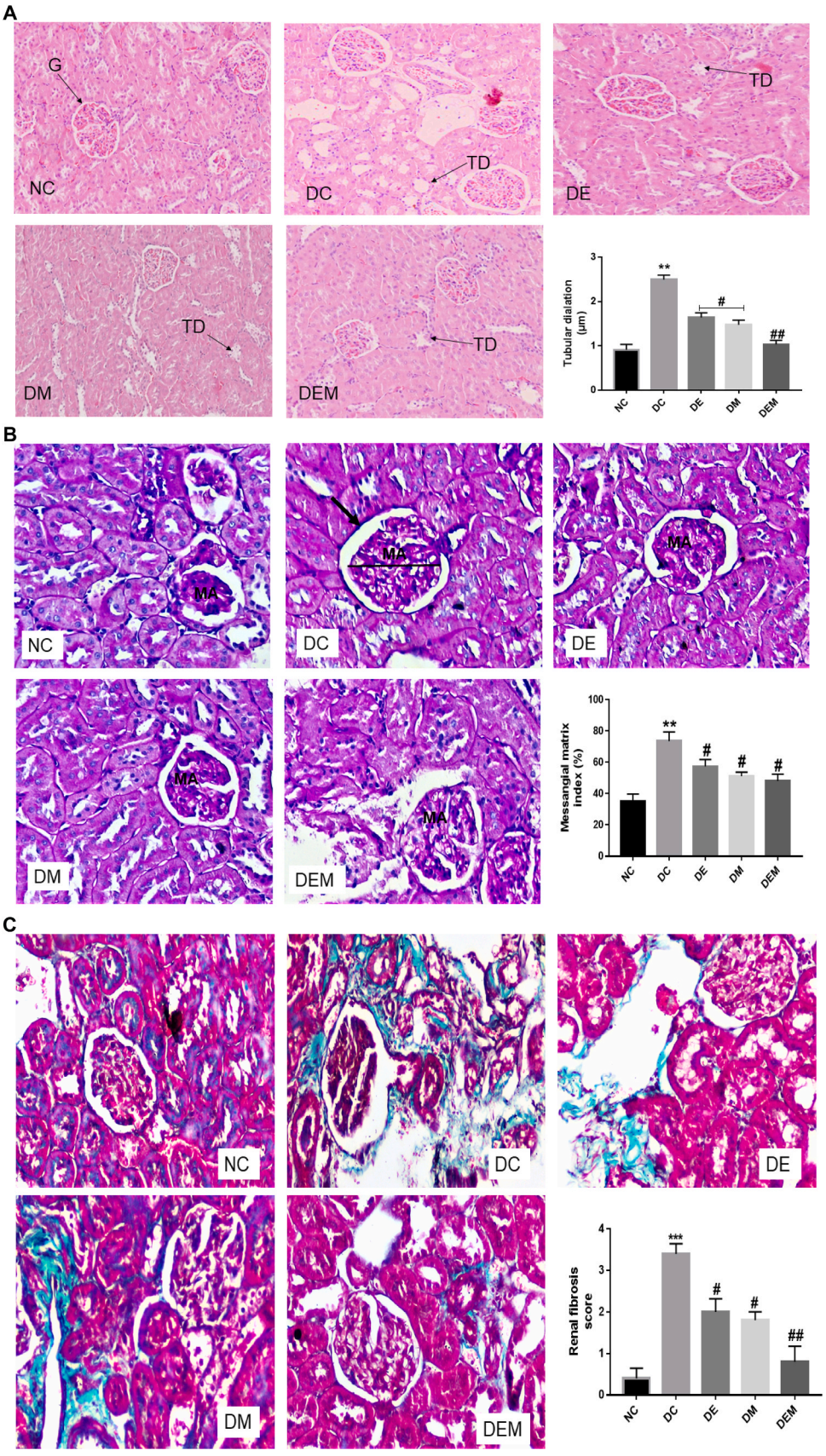

Fig. 8. (a). Photomicrographs of kidney sections stained with hematoxylin and eosin (x200; scale bar: 20 μm). NC rats showed normal renal histoarchitecture with normal size and morphology of the glomerulus and renal tubules. Compared to NC, the renal section in the DC rats showed dilation of the renal tubules (TD) with a slightly enlarged renal corpuscle. Kidney histology in the DE and DM rats showed mild tubular dilation, while coadministration of both L-egt and metformin to diabetic rats (DEM) prevent renal damage with a morphological structure similar to the NC rats. (b). Photomicrographs of kidney sections stained with PAS (x400; scale bar: 50 μm) and mesangial matrix index. NC rats showed kidney histology with a normal glomerular tuft and tubules. The histology of the DC rats showed glomerular hypertrophy with mesangial area (MA) expansion and diffuse thickening of the basement membrane (thick arrow). There is a reduction in the mesangial area with a normal glomerular tuft in all the treated diabetic groups compared to the DC group. (c). Photomicrographs of kidney sections stained with Masson trichrome stain (x400; scale bar: 50 μm) and renal fibrosis. The NC group showed normal renal interstitium. The DC rats showed renal fibrosis characterized by excess collagen deposit (green stain) in the renal interstitium, staining both the glomerular and tubular membrane. The DE and DM group showed mild fibrosis with a diffuse deposit of collagen in the renal interstitium. The kidney in the DEM group showed renal histology like the negative control (NC) with less collagen deposit in the renal interstitium. (For interpretation of the references to colour in this figure legend, the reader is referred to the web version of this article.)

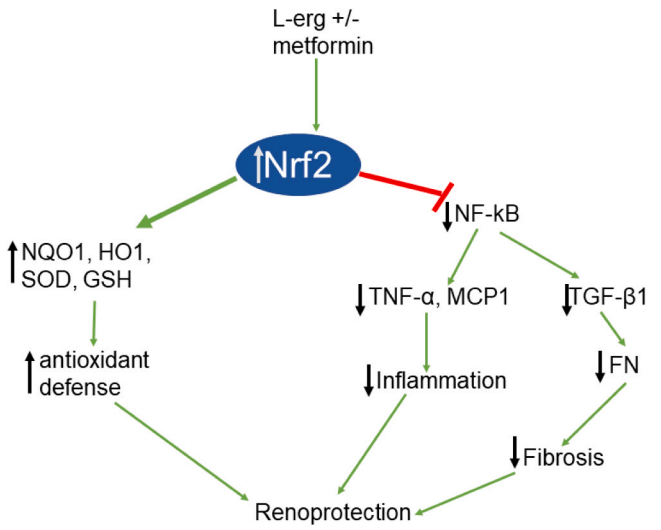

Fig. 9. Probable Reno-protective pathway of L-egt-induced Nrf2 activation. Nrf2 activation exerts two effects. 1) it upregulates the cytoprotective genes and antioxidant enzymes to enhance the antioxidant defense system. 2) it inhibits the NF-kB inflammatory gene to reduce inflammatory cytokines and downregulate TGF-β1 gene and its downstream fibrotic protein in the extracellular matrix. The improved antioxidant defense and reduced renal inflammation alleviate diabetes-induced renal damage. Red = inhibition while green- = activation. (For interpretation of the references to colour in this figure legend, the reader is referred to the web version of this article.)

35]. Previous studies have reported that the activation of the Nrf2 signaling pathway protects the kidney against oxidative injury by enhancing the antioxidant defense system [14,37,73]. In this study, L-egt-induced Nrf2 activation in non-diabetic and diabetic animals was confirmed by the upregulation of Nrf2 protein and gene expression, with subsequent upregulation of its downstream cytoprotective genes HO-1 and NQO-1 that act as the central effector of the L-egt-induced Nrf2 activation. Consequently, the increased antioxidant defense system caused a reduction in lipid peroxidation and increased SOD, CAT, and GSH that works synergistically to quench the harmful effect of free radicals in the renal cells. These results suggest that L-egt can activate the Nrf2 antioxidant pathway to reduce renal injury during diabetes. Furthermore, literature has shown that metformin alleviates renal oxidative damage in addition to its antihyperglycemic effect [5,47]. Therefore, the additive effect of L-egt with metformin may account for the improved biological response compared to the administration of either treatment alone. Notably, clinical trial with Nrf2 activator such bardoxolone methyl has been terminated due to its potential contribution to cardiac injury [9]. However, not all Nrf2 activators have been associated with cardiac failure, and studies are yet to report the adverse effect of ergothioneine. Furthermore, most studies on ergothioneine are still at the experimental phase, while there is an ongoing clinical trial assessing the therapeutic benefit of ergothioneine to delay cognitive decline. Therefore, further studies are still needed to translate the experimental data from the bench to the bedside, focusing on evaluating the adverse effect of ergothioneine-induced Nrf2 activation in clinical studies.

Literature has shown the significant role of inflammation in the pathogenesis of DN [15,33]. Both insulin resistance and hyperglycemia stimulate low-grade inflammation characterized by an increased circulating level of inflammatory cytokines (TNF-α), chemokines (MCP-1), and fibrotic factors (TGF-β1), with significant loss of renal function [33, 43]. In this study, the L-egt-induced Nrf2 activation is accompanied by a reduction in renal inflammation in diabetic rats, which was associated with the downregulation of NF-kB gene expression and reduced concentration of its downstream cytokines TNF-α and MCP-1 in the diabetic kidney. This result is in accordance with previous studies reporting that reported a significant reduction in NF-kB activity sequel to Nrf2 activation [62,64]. During diabetes, monocytes and immune cells infiltrate the renal cells to promote matrix expansion and mesangial proliferation [17]. Interestingly, monocyte infiltration significantly decreased in the L-egt-treated animals as evidenced by the reduced MCP-1 in the kidney homogenates suggesting the anti-inflammatory activity of L-egt to reduce renal inflammation. Besides, studies have shown that the reno-protective effect of metformin goes beyond its antihyperglycemic efficacy; metformin protects against renal inflammation by inhibiting the NF-kB transcription pathway, thereby preventing the release of inflammatory cytokines [23,31]. Therefore, synergistic administration of L-egt and metformin may exert a potent anti-inflammatory effect in renal tissues more than the administration of either L-egt or metformin alone. The protective effect of L-egt against diabetes-induced renal injury can also be attributed to the inhibition of TGF-β1, a potent profibrotic factor, via Nrf2 activation. In this study, L-egt administration decreased the concentration and gene expression of TGF-β1 in the kidney as well as downregulate its downstream protein, fibronectin expression, in the extracellular matrix of diabetic animals.

Histological examination of the kidney provides detailed insight into the structural architecture of the renal corpuscle and tubules. In this study, the glomerular hypertrophy, mesangial expansion, thickened basement membrane, tubular degeneration, and excessive collagen deposit (a biomarker of renal fibrosis) observed in the diabetic control group are characteristic features of early kidney injury associate with T2D, and these have also been reported in similar studies [29,40,47]. However, most of these structural derangements are reduced in the L-egt treated group, while synergistic treatment with L-egt and metformin prevents histological aberrations in the kidney. These results suggest that L-egt may reduce cellular injury to stabilize the structural derangements evident in the T2D kidney. These observations are further supported by other indices of renal function, including the reduction in albuminuria, KIM-1, TGF-β1, and oxidative injury evaluated in this study.

5. Conclusion

This study showed that the combination of L-egt and metformin to diabetic animals improves therapeutic benefits on renal dysfunctions compared to either treatment alone. This therapeutic outcome is associated with the activation Nrf2 antioxidant signal to improve renal structure and function. L-egt-induced Nrf2 activation upregulates antioxidant cytoprotective genes (HO-1 and NQO1) to enhance the antioxidant defense system. Also, Nrf2 can downregulate NF-kB, TGF-β1, and fibronectin expression to inhibit renal inflammation. Furthermore, the combination of L-egt with metformin in diabetic animals reduced hypertriglyceridemia and improves glucose homeostasis. Thus, these findings highlight the therapeutic benefits of L-egt, which can be explored to alleviate metabolic disorders and use as an adjuvant regimen in the management of renal dysfunctions associated with T2D. However, the in-vitro analysis and analysis of specific L-egt transporters could not be done due to limited funding. Thus, further studies may be required to evaluate the detailed mechanism of action of L-egt fully.

Funding

This work was supported by the College of Health Science (CHS), University of KwaZulu-Natal, South Africa (grant number: 640997).

CRediT authorship contribution statement

Ayobami Dare: Conceptualization, Methodology, Formal analysis, Data curation, Writing – original draft, and Funding acquisition. **Mahendra Channa**: Writing – review & editing, Supervision. **Anand Nadar**: Methodology, Writing – review & editing, Supervision.

Declaration of Competing Interest

The authors declared that there is no conflict of interest.

Acknowledgements

The authors thank Dr. Jean-Claude Yadan from Tetrahedron (Parc Technologique Biocitech 102 avenue Gaston Roussel, Romainville, F 93230, France) for providing pure L-ergothioneine used in this study. The authors also acknowledge the assistance received from the Biomedical Resource Unit, Westville Campus, University of KwaZulu-Natal (UKZN).

Appendix A. Supporting information

Supplementary data associated with this article can be found in the online version at doi:10.1016/j.biopha.2021.111921.

References

[1] H. Aebi, [13] Catalase in vitro. Methods in Enzymology, Academic Press, 1984.
[2] L. Agius, B. Ford, S. Chachra, The metformin mechanism on gluconeogenesis and ampk activation: the metabolite perspective, Int. J. Mol. Sci. 21 (2020) 3240–3259.
[3] P. Aguilar, P. Gallego, G. Falcóngarcía, O. Cremades, R. Torres, A. Salazar, J. del Campo, J. Bautista, Ergothioneine rich agaricus bisporus extracts decreases lipid accumulation induced by Oleic Acid in Hepg2 cells: possible implications in the treatment of nonalcoholic liver fatty disease, J. Food Sci. Nutr. 5 (2019).
[4] N. Al-Waili, H. Al-Waili, T. Al-Waili, K. Salom, Natural antioxidants in the treatment and prevention of diabetic nephropathy; a potential approach that warrants clinical trials, Redox Rep. 22 (2017) 99–118.
[5] A.A. Alhaider, H.M. Korashy, M.M. Sayed-Ahmed, M. Mobark, H. Kfoury, M. A. Mansour, Metformin attenuates streptozotocin-induced diabetic nephropathy in rats through modulation of oxidative stress genes expression, Chem. Biol. Interact. 192 (2011) 233–242.
[6] R.G. Amorim, G.D.S. Guedes, S.M.D.L. Vasconcelos, J.C.D.F. Santos, Kidney disease in diabetes mellitus: cross-linking between hyperglycemia, redox imbalance and inflammation, Arq. Bras. Cardiol. 112 (2019) 577–587.
[7] D. Bolignano, V. Cernaro, G. Gembillo, R. Baggetta, M. Buemi, G. D'Arrigo, Antioxidant agents for delaying diabetic kidney disease progression: a systematic review and meta-analysis, PLoS One 12 (2017), 0178699.
[8] K.G. Cardenas Ureña, J.C. Ramírez Nava, F.G. Márquez Celedonio, O.I. Salas Nolasco, J.E. Villegas Domínguez, C.N. Crespo-Cortés, Clinical efficacy of adjuvant therapy with hyperbaric oxygen in diabetic nephropathy, Undersea Hyperb. Med 47 (2020) 415–422.
[9] M.P. Chin, D. Wrolstad, G.L. Bakris, G.M. Chertow, D. de Zeeuw, A. Goldsberry, P. G. Linde, P.A. McCullough, J.J. Mcmurray, J. Wittes, C.J. Meyer, Risk factors for heart failure in patients with type 2 diabetes mellitus and stage 4 chronic kidney disease treated with bardoxolone methyl, J. Card. Fail 20 (2014) 953–958.
[10] A. Cohen-Bucay, G. Viswanathan, Urinary markers of glomerular injury in diabetic nephropathy, Int. J. Nephrol. 2012 (2012), 146987.
[11] A.J. Collins, R.N. Foley, D.T. Gilbertson, S.-C. Chen, United States Renal Data System public health surveillance of chronic kidney disease and end-stage renal disease, Kidney Int. Suppl. 5 (2015) 2–7.
[12] N. D'Onofrio, L. Servillo, A. Giovane, R. Casale, M. Vitiello, R. Marfella, G. Paolisso, M.L. Balestrieri, Ergothioneine oxidation in the protection against high-glucose induced endothelial senescence: Involvement of SIRT1 and SIRT6, Free Radic. Biol. Med. 96 (2016) 211–222.
[13] M. Deiana, A. Rosa, V. Casu, R. Piga, M. Assunta Dessi, O.I. Aruoma, L-ergothioneine modulates oxidative damage in the kidney and liver of rats in vivo: studies upon the profile of polyunsaturated fatty acids, Clin. Nutr. 23 (2004) 183–193.
[14] Y. Ding, H. Li, Y. Li, D. Liu, L. Zhang, T. Wang, T. Liu, L. Ma, Protective effects of grape seed proanthocyanidins on the kidneys of diabetic rats through the Nrf2 signalling pathway, Evid. Based Complement. Altern. Med. eCAM 2020 (2020), 5205903.
[15] J. Donate-Correa, C.M. Ferri, F. Sánchez-Quintana, A. Pérez-Castro, A. González-Luis, E. Martín-Núñez, C. Mora-Fernández, J.F. Navarro-González, Inflammatory cytokines in diabetic kidney disease: pathophysiologic and therapeutic implications, Front. Med. 7 (2020), 628289.
[16] G.L. Ellman, Tissue sulfhydryl groups, Arch. Biochem. Biophys. 82 (1959) 70–77.
[17] E. Galkina, K. Ley, Leukocyte recruitment and vascular injury in diabetic nephropathy, J. Am. Soc. Nephrol. 17 (2006) 368–377.
[18] A. Gil-Ramírez, D. Morales, C. Soler-Rivas, Molecular actions of hypocholesterolaemic compounds from edible mushrooms, Food Funct. 9 (2018) 53–69.
[19] M. Gyurászová, R. Gurecká, J. Bábíčková, Ľ. Tóthová, Oxidative stress in the pathophysiology of kidney disease: implications for noninvasive monitoring and identification of biomarkers, Oxid. Med. Cell. Longev. 2020 (2020), 5478708.
[20] S.L. Habib, Alterations in tubular epithelial cells in diabetic nephropathy, J. Nephrol. 26 (2013) 865–869.
[21] B. Halliwell, I.K. Cheah, C.L. Drum, Ergothioneine, an adaptive antioxidant for the protection of injured tissues? A hypothesis, Biochem. Biophys. Res. Commun. 470 (2016) 245–250.
[22] Y.-C. Hseu, Y. Vudhya Gowrisankar, X.-Z. Chen, Y.-C. Yang, H.-L. Yang, The antiaging activity of ergothioneine in UVA-irradiated human dermal fibroblasts via the inhibition of the AP-1 pathway and the activation of Nrf2-mediated antioxidant genes, Oxid. Med. Cell. Longev. 2020 (2020), 2576823.
[23] K. Isoda, J.L. Young, A. Zirlik, L.A. Macfarlane, N. Tsuboi, N. Gerdes, U. Schönbeck, P. Libby, Metformin inhibits proinflammatory responses and nuclear factor-kappaB in human vascular wall cells, Arterioscler. Thromb. Vasc. Biol. 26 (2006) 611–617.
[24] J.C. Jha, C. Banal, B.S. Chow, M.E. Cooper, K. Jandeleit-Dahm, Diabetes and kidney disease: role of oxidative stress, Antioxid. Redox Signal. 25 (2016) 657–684.
[25] X. Jiang, W. Meng, L. Li, Z. Meng, D. Wang, Adjuvant therapy with mushroom polysaccharides for diabetic complications, Front. Pharmacol. 11 (2020) 168, 168-168.
[26] C. Jihua, C. Cai, B. Xubin, Y. Yue, Effects of dexmedetomidine on the RhoA /ROCK/ Nox4 signaling pathway in renal fibrosis of diabetic rats, Open Med. 14 (2019) 890–898.
[27] D. Kawanami, K. Matoba, K. Utsunomiya, Dyslipidemia in diabetic nephropathy, Ren. Replace. Ther. 2 (2016) 16.
[28] H.J. Ko, J. Kim, M. Ahn, J.H. Kim, G.S. Lee, T. Shin, Ergothioneine alleviates senescence of fibroblasts induced by UVB damage of keratinocytes via activation of the Nrf2/HO-1 pathway and HSP70 in keratinocytes, Exp. Cell Res. 400 (2021), 112516.
[29] X. Liu, J. Ma, M.T. Hu, X.D. Dong, L.T. Xiang, Q.R. Gu, Z.Y. Du, S.M. Chen, G. R. Chen, [Protective effects of Curcumin analogue L6H4 on kidney from type 2 diabetic rats], Zhongguo Ying Yong Sheng Li Xue Za Zhi 33 (2017) 11–15.
[30] K.J. Livak, T.D. Schmittgen, Analysis of relative gene expression data using real-time quantitative PCR and the 2(-Delta Delta C(T)) Method, Methods 25 (2001) 402–408.
[31] J. Lu, J. Ji, H. Meng, D. Wang, B. Jiang, L. Liu, E. Randell, K. Adeli, Q.H. Meng, The protective effect and underlying mechanism of metformin on neointima formation in fructose-induced insulin resistant rats, Cardiovasc. Diabetol. 12 (2013) 58.
[32] S. Marklund, Pyrogallol auto-oxidation, in: R. Greenwald (Ed.), Handbook of Methods for Oxygen Radical Research, CRC Press, Boca Raton, FL, 1985.
[33] K. Matoba, Y. Takeda, Y. Nagai, D. Kawanami, K. Utsunomiya, R. Nishimura, Unraveling the role of inflammation in the pathogenesis of diabetic kidney disease, Int. J. Mol. Sci. 20 (2019) 3393.
[34] M.E. Meneses, M. Galicia-Castillo, A. Pérez-Herrera, R. Martínez, H. León, D. Martínez-Carrera, Traditional mushroom consumption associated to lower levels of triglycerides and blood pressure in an indigenous peasant community from Oaxaca, Mexico, Int J. Med. Mushrooms 22 (2020) 953–966.
[35] A.G. Miranda-Díaz, L. Pazarín-Villaseñor, F.G. Yanowsky-Escatell, J. Andrade-Sierra, Oxidative stress in diabetic nephropathy with early chronic kidney disease, J. Diabetes Res. 2016 (2016), 7047238.
[36] B.N. Mkhwanazi, M.R. Serumula, R.B. Myburg, F.R. van Heerden, C. T. Musabayane, Antioxidant effects of maslinic acid in livers, hearts and kidneys of streptozotocin-induced diabetic rats: effects on kidney function, Ren. Fail. 36 (2014) 419–431.
[37] M. Nezu, N. Suzuki, Roles of Nrf2 in protecting the kidney from oxidative damage, Int. J. Mol. Sci. 21 (2020) 2951.
[38] D.V. Nguyen, L.C. Shaw, M.B. Grant, Inflammation in the pathogenesis of microvascular complications in diabetes, Front. Endocrinol. 3 (2012) 170.
[39] J.M. O'Connell, S.M. Manson, Understanding the economic costs of diabetes and prediabetes and what we may learn about reducing the health and economic burden of these conditions, Diabetes Care 42 (2019) 1609–1611.
[40] M.J. Oza, Y.A. Kulkarni, Formononetin attenuates kidney damage in type 2 diabetic rats, Life Sci. 219 (2019) 109–121.
[41] S. Palazhy, V. Viswanathan, Lipid abnormalities in Type 2 diabetes mellitus patients with overt nephropathy, Diabetes Metab. J. 41 (2017) 128–134.
[42] B.D. Paul, S.H. Snyder, The unusual amino acid L-ergothioneine is a physiologic cytoprotectant, Cell Death Differ. 17 (2010) 1134–1140.
[43] R.E. Pérez-Morales, M.D. del Pino, J.M. Valdivielso, A. Ortiz, C. Mora-Fernández, J. F. Navarro-González, Inflammation in Diabetic Kidney Disease, Nephron 143 (2019) 12–16.
[44] D.W. Powell, D.N. Kenagy, S. Zheng, S.C. Coventry, J. Xu, L. Cai, E.C. Carlson, P. N. Epstein, Associations between structural and functional changes to the kidney in diabetic humans and mice, Life Sci. 93 (2013) 257–264.
[45] G.K. Rangan, G.H. Tesch, Quantification of renal pathology by image analysis, Nephrology 12 (2007) 553–558.
[46] G.K. Rangan, Y. Wang, Y.-C. Tay, D.C.H. Harris, Inhibition of nuclear factor-κB activation reduces cortical tubulointerstitial injury in proteinuric rats, Kidney Int. 56 (1999) 118–134.
[47] H. Ren, Y. Shao, C. Wu, X. Ma, C. Lv, Q. Wang, Metformin alleviates oxidative stress and enhances autophagy in diabetic kidney disease via AMPK/SIRT1-FoxO1 pathway, Mol. Cell. Endocrinol. 500 (2020), 110628.
[48] G.T. Russo, S. de Cosmo, F. Viazzi, A. Pacilli, A. Ceriello, S. Genovese, P. Guida, C. Giorda, D. Cucinotta, R. Pontremoli, P. Fioretto, Plasma triglycerides and HDL-C levels predict the development of diabetic kidney disease in subjects with type 2 diabetes: the AMD annals initiative, Diabetes Care 39 (2016) 2278–2287.
[49] S.A. Salama, H.A. Omar, Modulating NF-κB, MAPK, and PI3K/AKT signaling by ergothioneine attenuates iron overload-induced hepatocellular injury in rats, J. Biochem. Mol. Toxicol. 35 (2021) 22729.
[50] R. Saran, B. Robinson, K.C. Abbott, L.Y.C. Agodoa, N. Bhave, J. Bragg-Gresham, R. Balkrishnan, X. Dietrich, A. Eckard, P.W. Eggers, A. Gaipov, D. Gillen, D. Gipson,

S.M. Hailpern, Y.N. Hall, Y. Han, K. He, W. Herman, M. Heung, R.A. Hirth, D. Hutton, S.J. Jacobsen, Y. Jin, K. Kalantar-Zadeh, A. Kapke, C.P. Kovesdy, D. Lavallee, J. Leslie, K. McCullough, Z. Modi, M.Z. Molnar, M. Montez-Rath, H. Moradi, H. Morgenstern, P. Mukhopadhyay, B. Nallamothu, D.V. Nguyen, K. C. Norris, A.M. O'hare, Y. Obi, C. Park, J. Pearson, R. Pisoni, P.K. Potukuchi, P. Rao, K. Repeck, C.M. Rhee, J. Schrager, D.E. Schaubel, D.T. Selewski, S.F. Shaw, J.M. Shi, M. Shieu, J.J. Sim, M. Soohoo, D. Steffick, E. Streja, K. Sumida, M. K. Tamura, A. Tilea, L. Tong, D. Wang, M. Wang, K.J. Woodside, X. Xin, M. Yin, A. S. You, H. Zhou, V. Shahinian, US renal data system 2017 annual data report: epidemiology of kidney disease in the United States, Am. J. Kidney Dis. Off. J. Natl. Kidney Found. 71 (2018) 7 (A7-A7).

[51] S.M. Sheehan, R. Korstanje, Automatic glomerular identification and quantification of histological phenotypes using image analysis and machine learning, Am. J. Physiol. Ren. Physiol. 315 (2018) F1644–F1651.

[52] T.-Y. Song, N.-C. Yang, C.-L. Chen, T.L.V. Thi, Protective effects and possible mechanisms of ergothioneine and hispidin against methylglyoxal-induced injuries in rat pheochromocytoma cells, Oxid. Med. Cell. Longev. 2017 (2017), 4824371.

[53] T.Y. Song, H.C. Lin, C.L. Chen, J.H. Wu, J.W. Liao, M.L. Hu, Ergothioneine and melatonin attenuate oxidative stress and protect against learning and memory deficits in C57BL/6J mice treated with D-galactose, Free Radic. Res. 48 (2014) 1049–1060.

[54] K. Srinivasan, B. Viswanad, L. Asrat, C.L. Kaul, P. Ramarao, Combination of high-fat diet-fed and low-dose streptozotocin-treated rat: a model for type 2 diabetes and pharmacological screening, Pharm. Res. 52 (2005) 313–320.

[55] V.R. Stojanović, I.D. Jovanović, S.Z. Ugrenović, L.P. Vasović, V.S. Živković, M. V. Jocić, B.K. Kundalić, M.N. Pavlović, Morphometric analysis of nonsclerosed glomeruli size and connective tissue content during the aging process, Sci. World J. 2012 (2012), 845046.

[56] R.M.Y. Tang, I.K.-M. Cheah, T.S.K. Yew, B. Halliwell, Distribution and accumulation of dietary ergothioneine and its metabolites in mouse tissues, Sci. Rep. 8 (2018) 1601.

[57] J.A. Torres, M. Rezaei, C. Broderick, L. Lin, X. Wang, B. Hoppe, B.D. Cowley Jr., V. Savica, V.E. Torres, S. Khan, R.P. Holmes, M. Mrug, T. Weimbs, Crystal deposition triggers tubule dilation that accelerates cystogenesis in polycystic kidney disease, J. Clin. Investig. 129 (2019) 4506–4522.

[58] P.P. Toth, S. Philip, M. Hull, C. Granowitz, Elevated triglycerides (≥ 150 mg/dL) and high triglycerides (200–499 mg/dL) are significant predictors of hospitalization for new-onset kidney disease: a real-world analysis of high-risk statin-treated patients, Cardioren. Med. 9 (2019) 400–407.

[59] R. Trevisan, A.R. Dodesini, The hyperfiltering kidney in diabetes, Nephron 136 (2017) 277–280.

[60] D. Turck, J.-L. Bresson, B. Burlingame, T. Dean, S. Fairweather-Tait, M. Heinonen, K.I. Hirsch-Ernst, I. Mangelsdorf, H.J. Mcardle, A. Naska, M. Neuhäuser-Berthold, G. Nowicka, K. Pentieva, Y. Sanz, A. Siani, A. Sjödin, M. Stern, D. Tomé, M. Vinceti, P. Willatts, K.-H. Engel, R. Marchelli, A. Pöting, M. Poulsen, J.R. Schlatter, R. Ackerl, H. van Loveren, Statement on the safety of synthetic l-ergothioneine as a novel food – supplementary dietary exposure and safety assessment for infants and young children, pregnant and breastfeeding women, EFSA J. Eur. Food Saf. Auth. 15 (2017) 05060.

[61] V. Vallon, R. Komers, Pathophysiology of the diabetic kidney, Compr. Physiol. 1 (2011) 1175–1232.

[62] N. Wakabayashi, S.L. Slocum, J.J. Skoko, S. Shin, T.W. Kensler, When NRF2 talks, who's listening? Antioxid. Redox Signal. 13 (2010) 1649–1663.

[63] X. Wang, J. Li, L. Huo, Y. Feng, L. Ren, X. Yao, H. Jiang, R. Lv, M. Zhu, J. Chen, Clinical characteristics of diabetic nephropathy in patients with type 2 diabetic mellitus manifesting heavy proteinuria: a retrospective analysis of 220 cases, Diabetes Res. Clin. Pract. 157 (2019), 107874.

[64] J.D. Wardyn, A.H. Ponsford, C.M. Sanderson, Dissecting molecular cross-talk between Nrf2 and NF-κB response pathways, Biochem. Soc. Trans. 43 (2015) 621–626.

[65] A.M. Warren, S.T. Knudsen, M.E. Cooper, Diabetic nephropathy: an insight into molecular mechanisms and emerging therapies, Expert Opin. Ther. Targets 23 (2019) 579–591.

[66] A.J. Weigand-Heller, P.M. Kris-Etherton, R.B. Beelman, The bioavailability of ergothioneine from mushrooms (Agaricus bisporus) and the acute effects on antioxidant capacity and biomarkers of inflammation, Prev. Med. 54 (Suppl) (2012) S75–S78.

[67] R.D. Williamson, F.P. McCarthy, S. Manna, E. Groarke, D.B. Kell, L.C. Kenny, C. M. McCarthy, L-(+)-ergothioneine significantly improves the clinical characteristics of preeclampsia in the reduced uterine perfusion pressure rat model, Hypertension 75 (2020) 561–568.

[68] R.D. Wilson, M.S. Islam, Fructose-fed streptozotocin-injected rat: an alternative model for type 2 diabetes, Pharm. Rep. 64 (2012) 129–139.

[69] H. Xiao, J. Zhang, Z. Xu, Y. Feng, M. Zhang, J. Liu, R. Chen, J. Shen, J. Wu, Z. Lu, X. Fang, J. Li, Y. Zhang, Metformin is a novel suppressor for transforming growth factor (TGF)-β1, Sci. Rep. 6 (2016), 28597-28597.

[70] C.M. Yuan, R. Nee, K.A. Ceckowski, K.R. Knight, K.C. Abbott, Diabetic nephropathy as the cause of end-stage kidney disease reported on the medical evidence form CMS2728 at a single center, Clin. Kidney J. 10 (2017) 257–262.

[71] L. Zhai, S. Ye, J. Gu, D. Yang, W. Hu, [Protective effects of metformin on glomerular podocytes of type 2 diabetes model rats], Zhonghua Yi Xue Za Zhi 95 (2015) 3313–3316.

[72] J. Zhang, J. Liu, X. Qin, Advances in early biomarkers of diabetic nephropathy, Rev. Assoc. Méd. Bras. 64 (2018) 85–92.

[73] R. Zhang, M. Lu, S. Zhang, J. Liu, Renoprotective effects of Tilianin in diabetic rats through modulation of oxidative stress via Nrf2-Keap1 pathway and inflammation via TLR4/MAPK/NF-κB pathways, Int. Immunopharmacol. 88 (2020), 106967.